

Level mixing spectroscopy

F. Hardeman, G. Scheveneels, G. Neyens, R. Nouwen, G. S'heeren, M. Van Den Bergh, and
R. Coussement

Instituut voor Kern- en Stralingsfysika, Celestijnenlaan 200 D, B-3001 Leuven, Belgium

(Received 7 May 1990)

This paper intends to introduce the reader to a recent method of determining the static quadrupole interaction of isomers in solids: LEMS (level mixing spectroscopy). First of all, the basic principle of level mixing is explained, and it is shown how this phenomenon can be observed in the angular distribution of radiation emitted by the decaying isomer. Furthermore, LEMS is compared to level mixing resonances and time differential perturbed angular distribution. It is shown that LEMS is a very attractive method in cases where high spin states are involved, and for isomers with lifetimes up to several milliseconds.

INTRODUCTION

If one has a quick look at a survey of quadrupole moments so far,^{1,2} it can easily be seen that there is still a lack of experimental data in two important situations, namely, in the μs -s lifetime region and at high spins ($I > 15\hbar$). Several years ago, in order to overcome this problem, our Leuven group presented the theory³ and some results⁴ of LMR (level mixing resonances). Also, a more simplified theoretical description valid for in-beam experiments has been published.⁵ Although LMR is able indeed to be applied at longer lifetimes,⁴ it still appeared to be very difficult at very high spins. This problem is now overcome by the LEMS method (level mixing spectroscopy), which also works at high spins,⁶ and which is basically an extension of LMR.

In the first section, the basic principles of LEMS are explained while Sec. II discusses the observation of the level mixing effect. In the third section, a detailed comparison is made with LMR and TDPAD (time differential perturbed angular distribution), showing the advantages and disadvantages of all three methods. Finally, the typical experimental apparatus is described. A summary of the formalism needed to calculate LEMS curves is given in the Appendix.

I. LEVEL MIXING

The aim of the method is to study the static quadrupole interaction of isomers in solid hosts. For simplicity, only host materials with an axially symmetric electric-field gradient (e.g., hcp lattice) have been used so far. The axial symmetry axis is called the Z_{PAS} axis.

The Hamiltonian describing the quadrupole interaction in the PAS frame is given by

$$H_Q = \hbar\omega_Q \frac{1}{\hbar^2} (3I_{Z_{PAS}}^2 - I^2), \quad (1.1)$$

with

$$\omega_Q = \frac{eQV_{zz}}{\hbar 4I(2I-1)}.$$

Expressed in the $|Im\rangle$ basis, $|Im\rangle$ being the eigenstates of $I_{Z_{PAS}}$, it becomes

$$\langle Im | H_Q | Im' \rangle = \hbar\omega_Q [3m^2 - I(I+1)] \delta_{m,m'}. \quad (1.2)$$

Let us now add a magnetic dipole interaction to this Hamiltonian by applying an external magnetic field B . If B is parallel to Z_{PAS} , the total Hamiltonian $H_T = H_Q + H_B$ remains symmetric around the Z_{PAS} axis:

$$\begin{aligned} H_B &= -\mu B = -\frac{g\mu_N}{\hbar} I_{Z_{PAS}} B, \\ H_T &= -\omega_B I_{Z_{PAS}} + \omega_Q / \hbar (3I_{Z_{PAS}}^2 - I^2), \end{aligned} \quad (1.3)$$

with

$$\omega_B = \frac{g\mu_N B}{\hbar},$$

and expressed in the $|Im\rangle$ basis:

$$\langle Im | H_T | Im' \rangle = \{ -\hbar\omega_B m + \hbar\omega_Q [3m^2 - I(I+1)] \} \delta_{mm'}. \quad (1.4)$$

As soon as a misalignment angle β between the Z_{PAS} axis and B is present (Fig. 12), (1.3) and (1.4) are transformed to

$$\begin{aligned} H_T &= H_Q + H_{B_{\parallel}} + H_{B_{\perp}} \\ &= \frac{\omega_Q}{\hbar} (3I_{Z_{PAS}}^2 - I^2) - \omega_B \cos\beta I_{Z_{PAS}} + \omega_B \sin\beta I_{X_{PAS}} \\ &= \frac{\omega_Q}{\hbar} (3I_{Z_{PAS}}^2 - I^2) \end{aligned} \quad (1.5a)$$

$$- \omega_B \cos\beta I_{Z_{PAS}} + \omega_B \sin\beta \left[\frac{(I_+ + I_-)}{2} \right] \quad (1.5b)$$

and

$$\langle Im | H_T | Im \rangle = \hbar\omega_Q [3m^2 - I(I+1)] - \hbar\omega_Q m \cos\beta, \quad (1.6a)$$

$$\langle Im | H_T | Im - 1 \rangle = \frac{\hbar\omega_B}{2} \sin\beta [(I+m)(I-m+1)]^{1/2}, \quad (1.6b)$$

and all matrix elements

$$\langle Im | H | Im' \rangle \text{ with } |m - m'| \geq 2 \text{ are zero.}$$

In Fig. 1, an energy-level scheme of H_T is given for $\beta=0$. At zero field, one observes the well-known quadrupole splitting. At higher fields, it is lifted by the superimposed nuclear Zeeman splitting, and all degeneracies disappear, except at some equidistant magnetic fields given by $\omega_B/\omega_Q = 3n$ ($n = 1, \dots, 2I - 1$), where two levels cross each other. This can give rise to the so-called level crossing resonances (LCR), described in a previous paper.⁷ At very high fields, the quadrupole interaction becomes negligible (it is decoupled), and the energy splitting equals the nuclear Zeeman splitting.

In Fig. 2, a small misalignment angle β is present. The basic picture remains the same, except near the "crossing fields" of the collinear case. This means that the small component B_1 generally can be neglected, except near the crossing points. The level splitting caused by this misalignment is due to the (1.6b) matrix elements. This splitting can be calculated by higher-order perturbation theory as explained in Refs. 3 and 5. This nondiagonal part not only causes a splitting of the energy levels, but also involves a complete mixing of the $|Im\rangle$ states. If β is sufficiently small, only two $|Im\rangle$ states are mixed, and this gives rise to the level mixing resonances (LMR).³⁻⁵

If β is increased still further, three or more levels get mixed (Fig. 3). In this case, although one still has the quadrupole splitting at zero field and the decoupled Zeeman splitting at very high field, the intermediate region is much more complicated, and it is no longer possible to identify any $|Im\rangle$ states in the level scheme. However, if one manages to identify the region where the mixing is

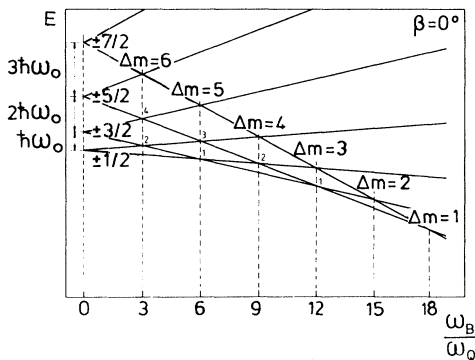


FIG. 1. Hyperfine energy-level scheme for a perfectly aligned magnetic dipole and axially symmetric electric quadrupole interaction as a function of ω_B/ω_Q .

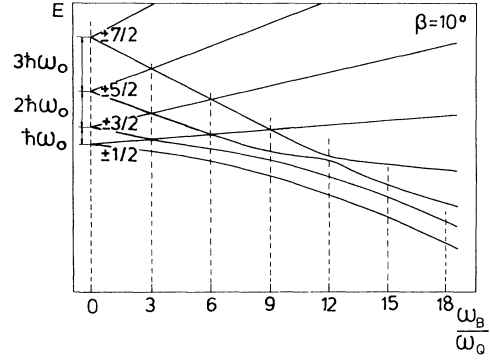


FIG. 2. Same as Fig. 1, but with a small misalignment angle β .

most important, one can still determine ω_Q/g , although with lower precision compared to LMR. If polycrystals are used, one needs to perform an integration over all possible angles between the Z_{PAS} axes and the magnetic field. This gives results similar as in the "large β " case. Due to the combined magnetic and quadrupole interaction strength a mixing of the energy levels occurs and therefore the method is called level mixing spectroscopy (LEMS). It can also be called a "decoupling" experiment as explained above.

II. OBSERVATION OF LEVEL MIXING

If the Hamiltonian (1.5) acts as an intermediate state perturbation, its influence can be studied by observing subsequent radiation of this state (Fig. 4). Just as in the LMR case, one observes the time-integrated perturbed angular distribution of the radiation⁸ given by

$$W(\theta, \phi, \tau) = \sqrt{4\pi} \sum_{kn} \hat{k}^{-1} A_k(R) B_k^n(\tau) Y_k^n(\theta, \phi), \quad (2.1)$$

with $A_k(R)$ being the radiation parameters of the observed transitions, $B_k^n(\tau)$ being the time-integrated orientation tensors, $Y_k^n(\theta, \phi)$ being the spherical harmonics describing the detection directions, and $\hat{k} = \sqrt{2k+1}$. The time-integrated orientation parameters are related to

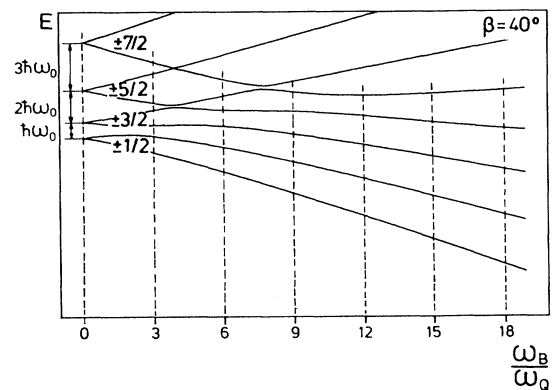


FIG. 3. Same as Fig. 2, but with a large misalignment angle β .

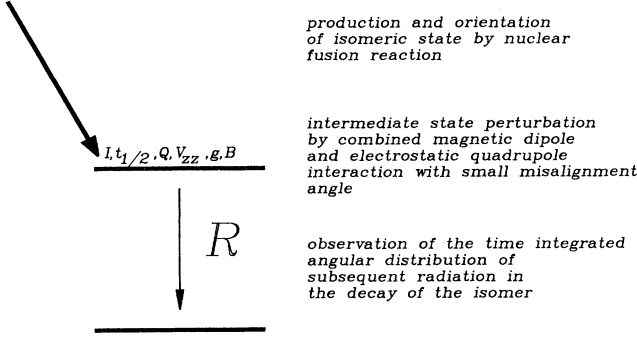


FIG. 4. Basic scheme of a LEMS experiment.

the initial orientation $B_k^q(t=0)$ by⁸

$$B_k^n(\tau) = \sum_{k'q} G_{kk'}^{nq}(\tau) B_{k'}^q(t=0). \quad (2.2)$$

The $G_{kk'}^{nq}(\tau)$ are called the time-integrated perturbation factors; they contain the influence of the Hamiltonian on the orientation of the levels, and have been integrated over time, including a $e^{-t/\tau}$ weight function to incorporate the nuclear lifetime of the isomer. Inserting (2.2) into (2.1), one obtains

$$W(\theta, \phi, \tau) = \sqrt{4\pi} \sum_{kn} \hat{k}^{-1} A_k \sum_{k'q} G_{kk'}^{nq}(\tau) B_{k'}^q(t=0) Y_k^n(\theta, \phi). \quad (2.3)$$

So, LEMS belongs to the so-called TIPAD techniques (time-integrated perturbed angular distribution). The initial orientation is obtained by the nuclear reaction and is described by the orientation tensors $B_k^q(I, t=0)$. As the orientation is axially symmetric around the beam axis, only the $q=0$ components are not vanishing and as only alignment is achieved, only $k'=\text{even}$ can occur.

In principle, one can select all possible angles between the beam axis and the magnetic field. In practice, one is limited to a parallel or a perpendicular configuration, due to split coil magnet construction requirements. In this paper, we only deal with the parallel geometry, unless explicitly mentioned (see Sec. IV B).

In case the magnetic field \mathbf{B} is parallel to the incident beam, the initial orientation is axially symmetric around the Z_{lab} axis; the Z_{PAS} axis makes an angle β with it, and the X_{lab} axis is chosen to be in the $Z_{\text{lab}}-Z_{\text{PAS}}$ plane. If one detects γ rays only, Eq. (2.3) can be simplified to the $k=\text{even}$ terms,⁸ and it reduces to

$$W(\theta, \phi, \tau) = \sum_{k,k'=2,4} \sum_n \sqrt{4\pi} \hat{k}^{-1} A_k G_{kk'}^{n0}(\tau) \times B_k^0(t=0) Y_k^n(\theta, \phi). \quad (2.4)$$

All the information about the Hamiltonian acting as an intermediate state perturbation is contained in the time-integrated perturbation factors $G_{kk'}^{n0}(\tau)$ which are a function of ω_B/ω_Q . As a function of the magnetic field they are difficult to describe; however, at zero field and at very

high fields they can be calculated analytically. In the intermediate-field range, numerical methods are needed.

A. The perturbation factors at zero magnetic field

At zero field, the only interaction being present is the quadrupole one; so it is easy to calculate $G_{kk'}^{nq}(\tau)$ in the PAS frame. As detection angles are described in the laboratory frame, a reference frame transformation needs to be performed.

It can be shown for sufficiently long lifetimes that $[G_{kk'}^{nq}(\tau)]_{\text{lab}}$ depends only on k, k' and β (see Appendix) but not on ω_Q, g , or τ . This means that the zero-field anisotropy is reduced (compared to the original one), to a value that can be calculated exactly if the angle β and the relative importance of the $k=2, 4, \dots$ terms in Eq. (2.4) are known.

For high spins, it can be shown that (see Appendix)

$$[G_{kk'}^{00}(\tau, B=0)]_{\text{lab}} \approx [P_k(\cos\beta)]^2 \delta_{kk'} \quad (2.5)$$

as illustrated in Fig. 5.

For polycrystalline samples, an average over all angles β needs to be made.⁸ For this case,

$$W(\theta, \phi, \tau, B=0, \text{poly}) = \sqrt{4\pi} \sum_k \hat{k}^{-1} A_k B_k^0(t=0) Y_k^0(\theta, \phi) \times \frac{1}{2k+1} \sum_q [G_{kk}^{qq}(\tau)]_{\text{PAS}}. \quad (2.6a)$$

For large spins, the $G_{kk}^{qq}(\tau)$ tend to $\delta_{q,0}$ (see Appendix), which reduces (2.4) to

$$W(\theta, \phi, \tau, B=0, \text{poly}) = \sqrt{4\pi} \sum_k \hat{k}^{-1} A_k B_k^0(t=0) Y_k^0(t=0) \frac{1}{2k+1}. \quad (2.6b)$$

This means that each component in the orientation is at-

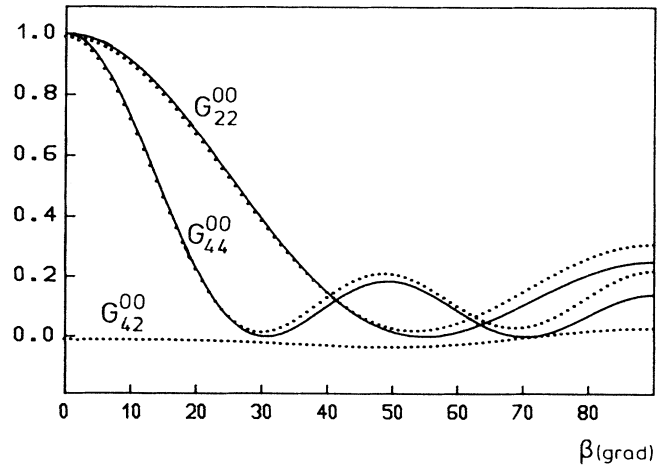


FIG. 5. Comparison between $[G_{kk}^{00}(\tau, B=0)]_{\text{lab}}$ (dotted lines) and $[P_k(\cos\beta)]^2$ (solid lines) for $k=2, 4$.

tenuated by a factor $1/(2k+1)$. If the relative importance of the $k=2,4,\dots$ terms is known, one can calculate exactly the zero-field anisotropy.

B. The perturbation factors at high field

At high field, the system is ruled by the strong magnetic interaction which has its symmetry axis parallel to the beam. This interaction causes a Larmor precession of the nuclear spins around the B axis which is a symmetry axis of the initial orientation. Therefore, the time-averaged orientation equals the initial one. Analytically, one finds

$$G_{kk}^{n0}(\tau, \text{high field} \parallel \text{beam}) = \delta_{kk} \delta_{n,0}. \quad (2.7)$$

C. Perturbation factors at intermediate fields

As it is impossible to calculate the G_{kk}^{nq} (τ, B intermediate) analytically, numerical calculations are necessary (see Fig. 6). If one looks at zero-field anisotropies for various angles β , one clearly sees that almost no attenuation occurs at small angles β ($[P_k(\cos\beta)]^2 \approx 1$); a maximum attenuation is obtained at about 55° . At high fields the anisotropy is saturated at a value that is the same for all angles. This high-field anisotropy corresponds to the completely decoupled case as described in the preceding paragraph. In the intermediate range, one obtains various types of curves, while for small β one can even still find small level mixing resonances. A curve representing the anisotropy change for a polycrystalline sample is shown in Fig. 7.

D. Variation with lifetime

The zero-field values and the curves in Figs. 6 and 7 are only valid if the lifetime is sufficiently long compared to the quadrupole interaction period ($\omega_Q \tau \gg 1$). Otherwise, the interaction does not have a sufficiently large period of time to reduce the anisotropy completely, and an intermediate value between 1 and Eq. (2.5) (high spins) or (2.6) (polycrystals) is obtained. This is discussed further in the paper (Sec. III C 1).

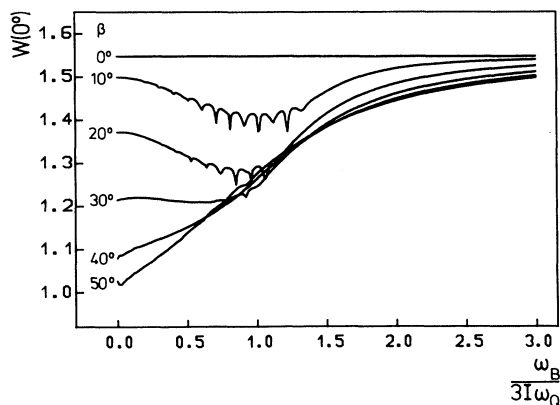


FIG. 6. Typical computer calculated LEMS curves for various angles of β for a spin-10 isomer.

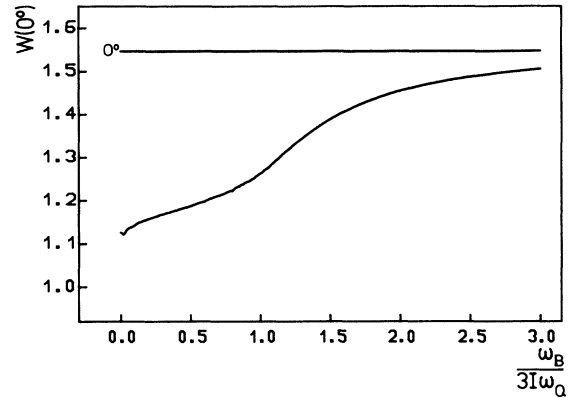


FIG. 7. Typical LEMS curve in a polycrystalline sample (spin 10).

E. Extraction of information from a LEMS curve

A precise determination of the high-field value $N(0^\circ)/N(90^\circ)$ (N being the number of counts at 0° or 90° with respect to B), together with the zero-field value, permits us to determine the initial alignment and to estimate the attenuation factors α_k defined by

$$B_k^0 = \alpha_k B_k^0 \quad (\text{maximum alignment}).$$

Describing the initial orientation after a nuclear reaction by a Gaussian distribution of the population over the $|Im\rangle$ states (as explained in Ref. 9), the high-field value $N(0^\circ)/N(90^\circ)$ gives rise to only one-fit parameter σ , σ being the width of the Gaussian curve. The zero-field value $N(0^\circ)/N(90^\circ)$ itself also contains information on detection efficiencies (detector efficiency, γ -ray absorption in the magnet, etc.).

One other difficulty may be the exact knowledge of the A_k parameters. Indeed, if multipolarity mixing takes place, δ is often unknown or uncertain. This requires that one more parameter needs to be determined. If the initial orientation can be determined, e.g., from other pure, nonperturbed transitions, the LEMS method can also be used to determine δ values. If only one transition is present, and if it is admixed, then care has to be taken to use this LEMS technique. It is perhaps useful to mention that δ or A_k parameters in the literature may be wrong if isomers are present in the decay scheme. Indeed, a small perturbation (e.g., by a defect quadrupole interaction) may cause an important reduction of the anisotropy (as described in Sec. IIA). This, of course, yields wrong A_k coefficients and, in the worst cases, wrong multipolarity assignments.

The A_k as well as the B_k^0 parameters mainly determine the amplitude of the LEMS curve, and their value is decisive for the feasibility of the method as they govern the statistical precision required to observe the LEMS curve. If the A_k parameters are known rather accurately, and if the α_k parameters are well determined from the anisotropy at high and low magnetic field, then it is easy to determine ω_Q/g numerically. This is done by performing a fit with theoretical LEMS curves to the data. A first rough

TABLE I. Comparison between TDPAD, LMR, and LEMS.

Quantity	TDPAD	LMR	LEMS
Timing	Yes	No	No
High spins	Difficult	Difficult	"Easy"
Measured quantity	$Q \cdot V_{zz}$	$Q \cdot V_{zz} / \mu$	$Q \cdot V_{zz} / \mu$
Statistics	"Hard"	"Hard"	"Easy"
Lifetime limits			
Lower	10–100 ns	100 ns	10–100 ns
Upper	μ s	ms	ms
Accuracy	1%	1%	5–10 %
Radiation damage	Very sensitive	Sensitive	Not very sensitive

estimate can be obtained easily, as the field at which the anisotropy is the average between low- and high-magnetic-field values corresponds roughly to $\omega_Q = \omega_B / 3I$.

III. COMPARISON TO OTHER METHODS

In this section the characteristics of LEMS are compared to those of TDPAD (time differential perturbed angular distribution) and LMR (level mixing resonances). A summary is given in Table I.

A. Timing

As one measures a time-integrated curve, no timing is required for LEMS and LMR. Nevertheless, from an experimental point of view it is often desirable to use pulsed production. By applying beam pulsation with a frequency of the order of the lifetime of the investigated isomer, it is possible to optimize the signal-to-noise ratio of photopeaks originating from this isomer. However, the stringent requirements of a TDPAC measurement are not required.

The influence of beam pulsation on the level mixing method can easily be calculated in the density matrix formalism.^{5,6} When the level mixing condition is fulfilled ($\nu_Q \tau / I \geq 0.6$), pulsed production has no influence on the level mixing method. In the opposite case, however, care has to be taken when analyzing the data: The pulsed production has a stroboscopic effect on the LEMS method. In practice, the production of the isomer and reduction of the background are most efficient when T_{on} (beam-on period) and T_{off} are of the order of the lifetime of the isomer of interest.

B. Spin

For high spins, many frequencies appear in the quadrupole interaction Hamiltonian. This often causes a cancellation of all structure in the time-precession pattern of the spins, except at multiples of the basic period. This makes TDPAD often difficult for high spin states (Fig. 8). LMR has the disadvantage that the amplitude of the resonances decreases drastically at high spins. Furthermore, more "crossing fields" and thus more resonances are present; therefore, even if one could measure resonances, identification of the $|Im\rangle$ states involved would be

difficult. As LEMS curves are almost independent of the spin the LEMS method remains relatively easy, even at high spins.

C. Lifetime range

1. Lower limit

The lower limit of TDPAD is governed by the fact that one needs to be able to measure during at least a part of one precession period. For typical quadrupole frequencies, this is of the order of tens of ns. In the case of LMR, the lower limit is higher (of the order of 100 ns typically). This is studied in detail in Ref. 5.

In the case of LEMS, the lower limit is governed by the fact that the interaction at zero field must be able to reduce the initial orientation sufficiently [$G_{22}(B=0)$

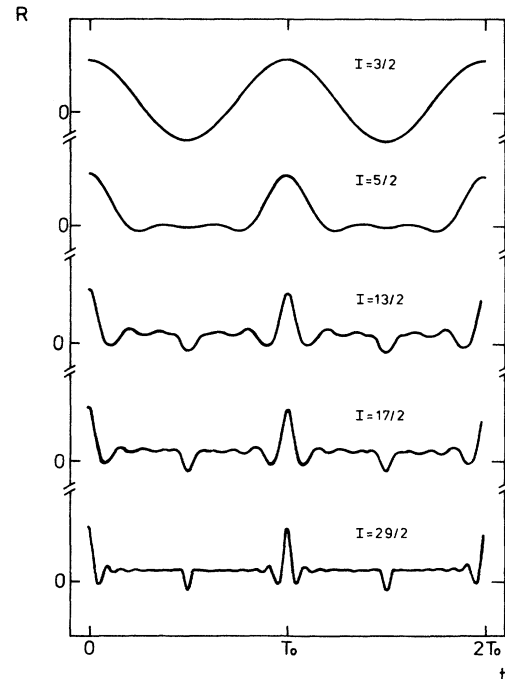


FIG. 8. TDPAD curves become hard to measure at high spin as the signal peaks become narrow if the spin is increased.

≤ 0.5]. This gives approximately the same lower limit as TDPAD (Fig. 9). For spins larger than ten, there is almost no difference between the curves $G_{22}(B=0)$ as a function of $\nu_Q\tau/I$, with $\nu_Q = eQV_{zz}/h$. One sees clearly that if $\nu_Q\tau/I \geq 0.6$, LEMS is possible. If it is smaller, one should also be careful if beam pulsing (see Sec. III A) is applied, as it can introduce stroboscopiclike effects in the LEMS curve. If $\nu_Q\tau/I \gg 0.6$, then beam pulsing does not influence the curve at all.

2. Upper limit

For TDPAD, the upper limit is caused by a loss of phase coherence between the spins, which introduces a damping of the modulation function $R(t)$. Furthermore, one has to deal with statistical problems. This usually results in an upper limit of a few μs . For LEMS, as well as for LMR, the limit is the spin lattice relaxation time. In practice, certainly at low temperatures, this is often of the order of several milliseconds or even seconds.

D. Measured quantity

TDPAD directly measures ν_Q , while LEMS and LMR determine ν_Q/g . The g factor of isomers suitable to LEMS or LMR is usually known by TDPAD (magnetic case) or NMR. (A wide range of externally applied magnetic fields is available to fulfill the condition of a TDPAD experiment.) For example, in the trans-lead region the g factors of high spin states up to $\frac{65}{2}\hbar$ are known in Bi (Ref. 12), At (Ref. 13), and Fr (Ref. 14) isotopes. It was possible to determine the quadrupole interaction frequency of several of these isomers by using the LEMS method. A discussion on these experimental LEMS results will be published in separate papers.

E. Target

LMR requires good-quality single crystals. LEMS and TDPAD can both use single crystals and polycrystalline

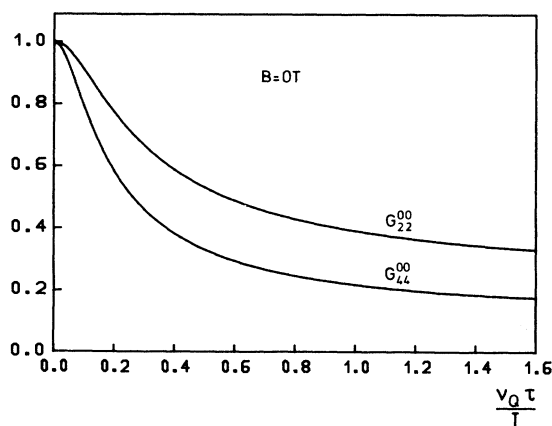


FIG. 9. The zero-field perturbation factor $G_{22}^{00}(\tau)$ for a polycrystal as a function of $\nu_Q\tau/I$. If $\nu_Q\tau/I$ is small, $G_{22}^{00}(\tau, B=0)$ tends to 1, and the amplitude of the corresponding LEMS curve is strongly reduced.

materials. In practice, the single-crystal experiments often give more precise and reliable results in both cases. Polycrystals are mainly used if enriched targets are needed.

F. Precision

The LEMS method is not a resonant method as are LMR and TDPAD. Therefore a LEMS experiment will be less accurate than a TDPAD or LMR experiment where precisions of 1% or better can be realized.

The accuracy on the quadrupole moment extracted from a LEMS curve depends on many parameters such as the g factor of the isomeric state, the knowledge of the electric-field gradient, the mixing ratio δ of the investigated transition, and so on. Therefore it has never been the purpose of a LEMS experiment to reach precisions better than 5%, which could be possible if we measured long enough.

By using a single-crystal host instead of a polycrystal, the accuracy of the experiment can be improved. When choosing the misalignment angle β around 40° , which corresponds to maximum change in anisotropy (see Fig. 6), an error of $\pm 2\%$ on β will have no effect on the extracted quadrupole frequency.

One uncertainty always present is the relative importance of the $A_2G_{22}B_2$, $A_2G_{24}B_4$, $A_4G_{42}B_2$, and $A_4G_{44}B_4$ terms, which all behave differently as a function of the magnetic field (Fig. 10). Usually, $A_2 \gg A_4$ and $B_2 \gg B_4$, but exceptions may occur. It can also be shown that the G_{24} components are negligible for high spins.

If there is doubt on the mixing ratio δ of an admixed transition, even more care about the relative importance needs to be taken. Usually, however, the zero-field and high-field values are sufficient to determine the relative importance of the ($k=4/k=2$) components with satisfactory precision. Knowledge of the absorption and detection efficiencies by normalizing to γ lines from radioactive decay can be useful.

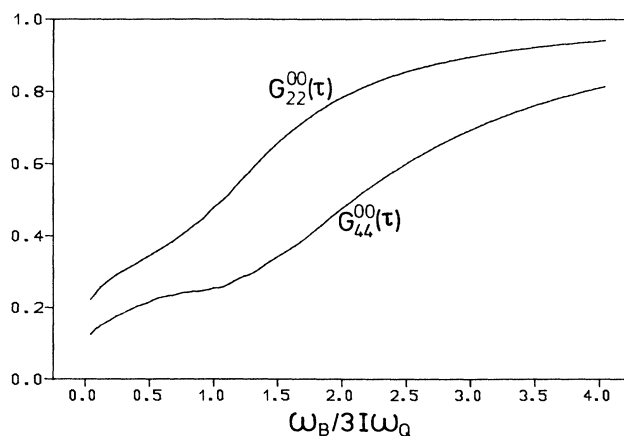


FIG. 10. Behavior of $G_{22}^{00}(\tau)$ and $G_{44}^{00}(\tau)$ as a function of B .

G. Radiation damage

With TDPAD, and to some extent with LMR too, one can obtain valuable information on radiation damage effects [e.g., the presence of distributions on the electric-field gradient (EFG)]. In TDPAD measurements, a spread on the EFG value causes a damping of the modulation as a function of time. In LMR, the narrow resonances are broadened and reduced in amplitude; however, one can reobtain the full resonance amplitude by tuning the misalignment angle β in such a way that the level mixing resonance linewidth is larger than the inhomogeneous broadening. This gives information about electric-field-gradient distributions.

A LEMS curve is virtually insensitive to this kind of effect: It is not possible to determine whether a Gaussian distribution on the field gradient is present or not. If there is a field-gradient distribution, the effect of it will be compensated: The LEMS curve for a larger EFG will compensate the one for the smaller EFG. A possible problem that could arise is radiation damage due to recoil of the beam into the target. However, in an hcp lattice the EFG felt by a nucleus on a substitutional site, free of defects, will be much lower (factor of 2 or more) than an electric-field gradient created by a defect in the near neighborhood of the investigated nucleus. Such difference in electric-field gradient can indeed be observed in our LEMS curves. Such effects¹⁵ were seen in the experiments on the ^{211,212,213}Fr isotopes in a Tl host and will be discussed in another paper. The accuracy on the quadrupole frequencies extracted from these experiments is of the order of 20%.

IV. EXPERIMENTAL SETUP

A. Parallel geometry

A schematic view of the LEMS setup as it is used by the Leuven group at the cyclotron Cyclone at Louvain-la-Neuve is shown in Fig. 11. This corresponds to the parallel geometry that has been described above. The beam impinges on a target which is mounted in the center of a superconducting split coil magnet. The target is either a polycrystal or a single crystal with its *c* axis making a large angle β (mostly around 40°) with respect to the beam axis. The magnetic field is parallel to the beam. Typical field strengths needed are of the order of 5

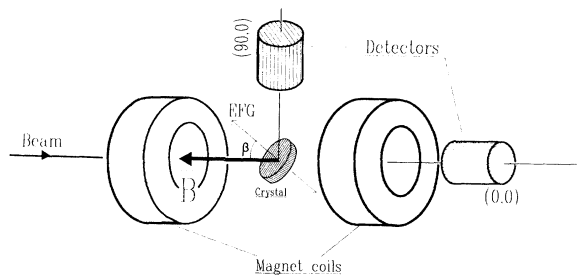


FIG. 11. Experimental setup in a parallel geometry.

T, with a homogeneity of 0.5% or better over the beam spot. The excited nuclei recoil into a host providing an EFG (often the target itself). Radiation is measured both parallel and perpendicular to the beam. If one does not have an annular γ -ray detector, the beam has to be stopped in the target. The ratio $N(0^\circ)/N(90^\circ)$ is measured as a function of B , in order to cancel beam intensity fluctuations. Experimental results will be published separately.

Advantages of this geometry are the fact that the largest amplitudes can be obtained this way; it is also the simplest one concerning beam optics. Disadvantages are the large background, x ray, and *n* flux as the target also serves as a beam stop.

It is worth mentioning that not all Ge detectors will work in the stray field of a magnet. This can sometimes be improved by reducing their bias voltage or by using a shielding but peak shape changes or even a detector breakdown as a function of the magnetic field may occur.

B. Perpendicular geometry

It is also possible to use a geometry in which the beam direction is perpendicular to the magnetic-field axis. This has the advantage that both the 0° and 90° detectors can be placed outside the beam direction. This can drastically clean the spectra.

At zero field, and for polycrystals, the beam axis is still a symmetry axis. This implies that $W(0^\circ) = W(90^\circ)$ (all angles refer to the magnetic-field system). So, the zero-field value works as a relative efficiency determination.

The main problem in this situation is the fact that the beam deviates in the magnetic field. For symmetric superconducting split coil magnets, the beam always impinges on the center of the target if everything is adjusted well.¹⁰ (The deviation in this stray field of the magnet compensates the deviation due to the central field.) For typical beams such as ¹²C⁴⁺, ¹⁴N⁴⁺ ($E = 80\text{--}90$ MeV) the maximum deviation of the beam (at $B = 5$ T) is about 12 mm; the angle of incidence on the target is 18°. The incident angle varies as a function of the applied field B , which causes a change in initial orientation as a function of B . This certainly should be taken into account very precisely. In principle, it should not induce any further uncertainties, but only makes analysis more complex. It may be that this geometry is favorable in many cases. This needs to be explored further more carefully.

V. CONCLUSION

If one can determine the orientation that originates from the nuclear reaction sufficiently well and if the isomer decays through at least one known transition (pure, or δ known), LEMS is a very good method to determine the quadrupole interaction strength of isomers in a solid host.

Its main advantages are that it works in a broad lifetime range, without restriction on the spin, and it is fast (the statistical precision required is less than that for the TDPAD method). Less favorable is the reduced precision (5–10%) and a relative insensitivity to small electric-field-gradient distributions.

Thus LEMS is to be preferred in the μs – ms lifetime region and if spins larger than $10\hbar$ are involved. Even if both TDPAD and LEMS are applicable, LEMS is often useful as it is a very fast method (runs of 30 h) which can rapidly give a good estimate of the quadrupole frequency ν_Q in many cases.

The authors wish to thank Dr. A. P. Byrne for his helpful comments on this text.

APPENDIX: FORMALISM NEEDED TO DESCRIBE LEMS

Although it may be easier for numerical calculations to work directly with the density matrix (as is done in Ref. 5), it is preferred here to use the orientation tensors and perturbation factors to describe LEMS. The time evolution of a density matrix is given by¹¹

$$i\hbar \frac{d\rho(I,t)}{dt} = [H(t), \rho(I,t)] . \quad (\text{A1})$$

For static Hamiltonians H , a solution for (A1) is

$$\rho(I,t) = \Lambda(t)\rho(I,t=0)\Lambda^\dagger(t) , \quad (\text{A2a})$$

with

$$\Lambda(t) = \exp(-iHt/\hbar) . \quad (\text{A2b})$$

The orientation tensors $B_k^n(I,t)$ are given by

$$B_k^n(I,t) = \hat{I} \hat{k} \sum_m (-)^{I+m} \begin{bmatrix} I & I & k \\ -m & m' & n \end{bmatrix} \langle Im | \rho(I) | Im' \rangle \quad (\text{A3})$$

$$G_{kk'}^{nq}(t) = \hat{k} \hat{k}' \sum_{m\mu} \sum_{NN'} (-)^{m-\mu} \begin{bmatrix} I & I & k \\ -m & m' & n \end{bmatrix} \begin{bmatrix} I & I & k' \\ -\mu & \mu' & q \end{bmatrix} \exp(-i\omega_{NN'}t) \langle m | N \rangle \langle N | \mu \rangle \langle m' | N' \rangle^* \langle N' | \mu' \rangle^* , \quad (\text{A6})$$

with $|m\rangle$, $|m'\rangle$, $|\mu\rangle$, $|\mu'\rangle$ being the eigenstates of the I_z operator with respect to some axis, $|N\rangle$, $|N'\rangle$ being the eigenstates of the Hamiltonian, $\omega_{NN'} = (E_N - E_{N'})/\hbar$, and $\hat{k} = \sqrt{2k+1}$.

If a time integration is performed, one defines

$$G_{kk'}^{nq}(\tau) = \int_0^\infty e^{-t/\tau} G_{kk'}^{nq}(t) dt / \int_0^\infty e^{-t/\tau} dt . \quad (\text{A7})$$

The exponentials take into account the nuclear decay of the isomer. One can easily derive that

$$G_{kk'}^{nq}(\tau) = \hat{k} \hat{k}' \sum_{m\mu} \sum_{NN'} (-)^{m-\mu} \begin{bmatrix} I & I & k \\ -m & m' & n \end{bmatrix} \begin{bmatrix} I & I & k' \\ -\mu & \mu' & q \end{bmatrix} \frac{1 - i\omega_{NN'}\tau}{1 + (\omega_{NN'}\tau)^2} \langle m | N \rangle \langle N | \mu \rangle \langle m' | N' \rangle^* \langle N' | \mu' \rangle^* . \quad (\text{A8})$$

In the case of LEMS, three axes are very important: (a) the Z_{PAS} axis, corresponding to the symmetry axis of the electric field gradient; (b) the magnetic-field axis, called Z_{lab} axis; the detection positions are described with respect to this axis; $\Phi=0$ can be taken to correspond to the $(Z_{\text{PAS}}, Z_{\text{lab}})$ plane; (c) the initial orientation (i.e., beam axis), called Z_{or} . Throughout this paper, it has been assumed that $Z_{\text{or}} = Z_{\text{lab}}$, which simplifies the method. If this is not the case (see, e.g., Sec. IV B), the angle between them must be taken into account.

The most general case is shown in Fig. 12. The transformation $\text{lab} \rightarrow \text{or}$ is described by $(\alpha, \beta, 0)$; it is possible to take

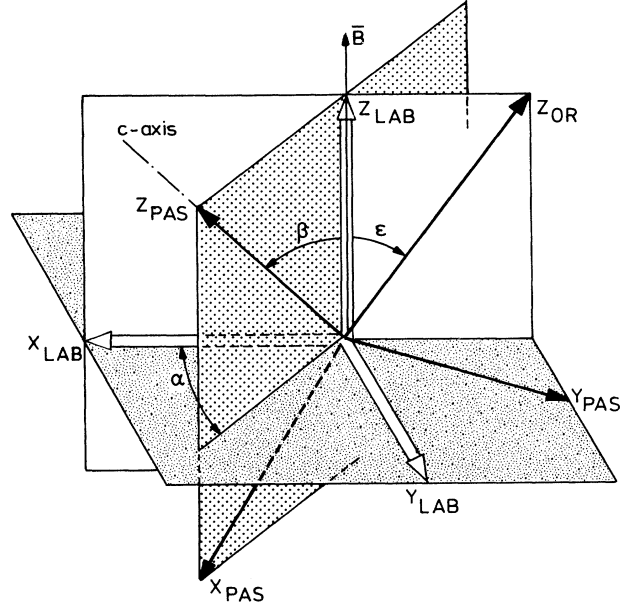


FIG. 12. Definition of the angles used in this paper.

with $\hat{x} = \sqrt{2x+1}$, and the inverse relation

$$\langle Im | \rho(I,t) | Im' \rangle = I^{-1} \sum_k \hat{k} (-)^{I+m} \begin{bmatrix} I & I & k \\ -m & m' & n \end{bmatrix} B_k^n(I) . \quad (\text{A4})$$

By inserting (A4) and (A3) into (A2), one finds

$$B_k^n(I,t) = \sum_{k'q} G_{kk'}^{nq} B_{k'}^q(I,t=0) , \quad (\text{A5})$$

with

$\alpha=0$ due to the axial symmetry of the magnetic field and the electric-field gradient. The angle ε , needed to transform the Z_{or} axis into the Z_{lab} axis, equals 0° in the geometry described in this paper, or 90° for the perpendicular geometry.

With the angles chosen as in Fig. 12, one can show that

$$[B_k^g(t)]_{\text{PAS}} = \sqrt{4\pi k'^{-1}} \sum_{q'} d_{qq'}^{k'}(-\beta) e^{iq'\alpha} Y_{k'}^{q'}(\varepsilon, 0) [B_k(t)]_{\text{or}} \quad (\text{A9a})$$

and

$$[B_k^g(t)]_{\text{PAS}} = \sum_{q'} d_{qq'}^{k'}(-\beta) e^{iq'\alpha} [B_k^g(t)]_{\text{lab}} \quad (\text{A9b})$$

[(A9b) is the simplification of (A9a) if $\varepsilon=0^\circ$]. The inverse relation of (A9b), which is

$$[B_k^g(t=0)]_{\text{lab}} = \sum_q d_{q'q}^{k'}(+\beta) e^{-iq\alpha} [B_k^g(t=0)]_{\text{PAS}}, \quad (\text{A10})$$

is necessary to express the $[G_{kk'}^{nq}(t)]_{\text{lab}}$ as a function of $[G_{kk'}^{nq}(t)]_{\text{PAS}}$:

$$[G_{kk'}^{nq''}(t)]_{\text{lab}} = \sum_{qq'} d_{nq}^k(\beta) d_{q'q}^{k'}(-\beta) e^{i(q''-q)\alpha} [G_{kk'}^{qq'}(t)]_{\text{PAS}}. \quad (\text{A11})$$

The same relation (A11) holds for the $G_{kk'}^{nq''}(\tau)$.

Calculation of the $G_{kk'}^{nq}(\tau, B=0)$ in the laboratory system

(This is also the orientation reference frame as the beam axis coincides with the magnetic field.)

At zero field, only the quadrupole interaction is present, and the perturbation factors are very simple in the PAS system. With axial symmetry, the $|m\rangle$ and $|N\rangle$ states coincide, and the energies are degenerate in $\pm m$.

The time-integrated perturbation factors for an axially symmetric quadrupole interaction in the PAS frame have been calculated by Steffen and Alder.⁸ In general, the result is rather complex, but under the assumption that $\omega_Q\tau \gg 1$, they simply reduce to

$$[G_{kk'}^{qq'}(B=0)]_{\text{PAS}} = \begin{cases} \delta_{kk'}\delta_{qq'} & \text{for } q=0, \\ \delta_{qq'}[1+(-)^{k+k'}] \begin{bmatrix} I & I & k \\ -q/2 & -q/2 & q \end{bmatrix} \begin{bmatrix} I & I & k' \\ -q/2 & -q/2 & q \end{bmatrix} & \text{for } q \neq 0. \end{cases} \quad (\text{A12a})$$

$$(\text{A12b})$$

For high spins, all terms (A12b) vanish, and the

$$[G_{kk'}^{qq'}(\tau, B=0)]_{\text{PAS}} = \delta_{kk'}\delta_{qq'}\delta_{q,0} \quad (\text{A13})$$

for high spins.

Using Eqs. (A13) and (A11), it is easily shown that

$$[G_{kk'}^{00}(\tau, B=0)]_{\text{lab}} = \delta_{kk'} [P_k(\cos\beta)]^2 \quad (\text{A14})$$

for high spins. In the polycrystalline case, the $[G_{kk'}^{qq'}(\tau, B=0)]_{\text{PAS}}$ are given by⁸ (if $\omega_Q\tau \gg 1$)

$$[G_{kk'}^{qq'}(\tau, B=0, \text{poly})]_{\text{lab}} = \delta_{q,q'}\delta_{q,0}\delta_{k,k'} \left[\frac{1}{2k+1} + \sum_{m=0} \begin{bmatrix} I & I & k \\ -m & -m & 2m \end{bmatrix}^2 \right]. \quad (\text{A15})$$

It can be shown that for $k=2$, (A15) reduces to $\frac{1}{5}$ for half-integer spins, and to a larger value for integer spins. However, as spin increases, this hard-core value approaches $\frac{1}{5}$ too, and one can conclude that

$$[G_{22}^{00}(\tau, B=0, \text{poly})]_{\text{lab}} = \frac{1}{5} \quad (\text{A16})$$

for high integer and for half-integer spins.

For high spins, it was shown that $G_{24}(\tau) = G_{42}(\tau) = 0$ [Eq. (A14)] at zero magnetic field; in the opposite case, when the magnetic interaction is sufficiently strong to decouple the quadrupole one, also $G_{24}(\tau) = G_{42}(\tau) = 0$ is obtained. In the intermediate-field range, it is preferable to use numerical calculations; they reveal that $G_{24}(\tau) \approx 0$ for all magnetic-field values for sufficiently high spin.

- ¹*Table of Isotopes*, edited by C. M. Lederer and V. S. Shirley (Wiley, New York, 1978); I. Berkes, in *Low-Temperature Nuclear Orientation*, edited by N. J. Stone and H. Postma (North-Holland, Amsterdam, 1986), p. 940.
- ²P. Raghavan, *At. Data Nucl. Data Tables* **42**, 189 (1989).
- ³R. Coussement, P. Put, G. Scheveneels, and F. Hardeman, *Hyperfine Interact.* **23**, 273 (1985).
- ⁴P. Put, R. Coussement, G. Scheveneels, F. Hardeman, I. Berkes, B. Hlimi, G. Marest, J. Sau, and E. H. Sayouty, *Phys. Lett.* **103A**, 151 (1984); I. Berkes, B. Hlimi, G. Marest, E. H. Sayouty, R. Coussement, F. Hardeman, P. Put, and G. Scheveneels, *Phys. Rev. C* **30**, 2026 (1984).
- ⁵G. Scheveneels, F. Hardeman, G. Neyens, and R. Coussement, *Hyperfine Interact.* **52**, 257 (1989).
- ⁶G. Scheveneels, Ph.D. thesis, K. U. Leuven, 1988.
- ⁷S. Shibuya, M. Fujioka, N. Kawamura, A. Matsumoto, S. Hayashibe, Y. Kimura, T. Ishimatsu, R. Coussement, M. Rots, L. Hermans, and P. Put, *Hyperfine Interact.* **14**, 315 (1983).
- ⁸R. M. Steffen and K. Alder, in *The Electromagnetic Interaction in Nuclear Spectroscopy*, edited by W. D. Hamilton (North-Holland, Amsterdam, 1975), p. 505.
- ⁹H. Morinaga and T. Yamazaki, *In-Beam Gamma-Ray Spectroscopy* (North-Holland, Amsterdam, 1970).
- ¹⁰H. H. Bertschat, private communication.
- ¹¹A. Messiah, *Mécanique Quantique* (Dunod, Paris, 1960).
- ¹²A. Kleinrahm, C. Günther, H. Hübel, B. V. Thirumala Rao, and R. Broda, *Nucl. Phys.* **A436**, 324 (1980).
- ¹³I. Bergström, J. Blomqvist, P. Carlé, B. Fant, A. Källberg, L. O. Norlin, K.-G. Rensfelt, and U. Rosengard, *Phys. Scr.* **31**, 333 (1985).
- ¹⁴A. P. Byrne, G. D. Dracoulis, C. Fahlander, H. Hübel, A. R. Poletti, A. E. Stuchberry, J. Gerl, R. F. Daire, and S. J. Poletti, *Nucl. Phys.* **A448**, 137 (1986).
- ¹⁵F. Hardeman, Ph.D. thesis, K. U. Leuven, 1989 (unpublished).